Indicator-Loaded Permeation-Selective Microbeads for Use in Fiber Optic Simultaneous Sensing of pH and Dissolved Oxygen

Ganna S. Vasylevska,[†] Sergey M. Borisov,[†] Christian Krause,[‡] and Otto S. Wolfbeis*[,†]

University of Regensburg, Institute of Analytical Chemistry, Chemo- and Biosensors, D-93040 Regensburg, Germany, and PreSens GmbH, Josef-Engert-Str. 11, D-93053 Regensburg, Germany

Received April 26, 2006. Revised Manuscript Received July 6, 2006

New materials are described that lead to sensors capable of simultaneous sensing of pH and oxygen via a single-fiber optic sensor. They make use of a pH probe based on carboxyfluorescein, and of a ruthenium(II) complex acting as a probe for dissolved oxygen. The selectivity of the probes was considerably improved by incorporating them into two kinds of microparticles, each of specific permeation selectivity. The pH probe was immobilized on particles made from proton permeable amino-modified poly(hydroxyethyl methacrylate), while the oxygen probe was physically immobilized in beads made from an organically modified sol−gel. Both kinds of beads were then dispersed into a hydrogel matrix and placed at the distal end of an optical fiber waveguide for optical interrogation. A phase-modulated blue-green LED serves as the light source for exciting luminescence whose average decay times or phase shifts serve as the analytical information. Data are evaluated by a modified dual luminophore referencing (m-DLR) method which relates the phase shift (as measured at two different frequencies) to pH and to oxygen partial pressure. The dually sensing material performs best if the sensing matrix is very homogeneous and if the microbeads have a diameter of $<3\ \mu$m.

1. Introduction

Oxygen and pH are key parameters in many areas of technology and research and are needed, for example, to control the quality of drinking water,[1,2] the freshness of food,[3−7] or the optimum reaction conditions for monitoring cell activity in bioreactors.[8−12] Knowing pH and oxygen concentration is also essential in clinical analysis of samples such as blood and other physiological liquids,[13−16] in seawater analysis,[17,18] and in marine research.[19−21] So far, pH and oxygen have been determined simultaneously via two sensors operated in parallel, which often is difficult for space limitations and in terms of sample volumes available. Hence, a sensor enabling simultaneous monitoring of both parameters would represent a powerful tool in various areas of research and in (bio)technology.

Most optical chemical sensors for noncolored and nonfluorescent species (including pH and oxygen) are based on the optical interrogation of a material that undergoes a change in its optical properties on exposure to the analyte of interest. Such a change is referred to as the response of the material and ideally is specific for the species to be sensed. In most cases, the sensor material is composed of an indicator dye contained in an optically transparent polymer. The polymer not only acts as a solvent for the (often fluorescent) indicator dye but also allows for the fine-tuning of the response curve of the indicator (and thus of the sensing range). The polymer also can provide certain permeation selectivity, thus eliminating cross-sensitivity to other species. All known indicator-based sensors for gases, for example, are based on materials that are impermeable to charged species (ions) that may act as quenchers of fluorescence.

Optical sensors nowadays can be miniaturized down to sub-micrometer dimensions and combined with fiber-optic technology to provide noninvasive[22,23] or remote measure-

* To whom correspondence should be addressed. Fax: +49-941-943-4064. Email: otto.wolfbeis@chemie.uni-regensburg.de.
[†] University of Regensburg.
[‡] PreSens GmbH.

(1) Canete, F.; Rios, A.; Luque de Castro, M. D.; Valcarcel, M. *Analyst* **1987**, *112*, 263.
(2) Preininger, C.; Klimant, I.; Wolfbeis, O. S. *Anal. Chem.* **1994**, *66*, 1841.
(3) John, G. T.; Goelling, D.; Klimant, I.; Schneider, H.; Heinzle, E. *J. Dairy Res.* **2003**, *70*, 327.
(4) Marshall, A. J.; Blyth, J.; Davidson, C. A. B.; Lowe, C. R. *Anal. Chem.* **2003**, *75*, 4423.
(5) Young, O. A.; Thomson, R. D.; Merhtens, V. G.; Loeffen, M. P. F. *Meat Sci.* **2004**, *67*, 107.
(6) O'Mahony, F. C.; O'Riordan, T. C.; Papkovskaya, N.; Kerry, J. P.; Papkovsky, D. B. *Food Control.* **2006**, *17*, 286.
(7) Papkovsky, D. B.; Papkovskaya, N.; Smyth, A.; Kerry, J.; Ogurtsov, V. I. *Anal. Lett.* **2000**, *33*, 1755.
(8) Masayasu, S.; Hiroaki, N.; Masaru, H. *Chem. Sens.* **2004**, *20*, 562.
(9) Deshpande, R. R.; Koch-Kirsch, Y.; Maas, R.; Krause, C.; Heinzle, E. *Assay Drug. Dev. Technol.* **2005**, *3*, 299.
(10) O'Mahony, F. C. *Environ. Sci. Technol.* **2005**, *39*, 5010.
(11) Alderman, J. *Biosens. Bioelectron.* **2004**, *19*, 1529.
(12) O'Donovan, C.; Hynes, J.; Yashunski, D.; Papkovsky, D. B. *J. Mater. Chem.* **2005**, *15*, 2946.
(13) Shimpey, K.; Hiroaki, S. *Chem. Sens.* **2003**, *19*, 25.
(14) Jeevarajan, A. S.; Vani, S.; Tazlor, T. D.; Anderson, M. M. *Biotechnol. Bioeng.* **2002**, *78*, 467.
(15) Mekhail, K.; Khacho, M.; Gunaratnam, L.; Lee, S. *Cell Cycle* **2004**, *3*, 1027.
(16) Meruva, R. K.; Meyerhoff, M. E. *Biosens. Bioelectron.* **1998**, *13*, 201.
(17) Bellerby, R. G.; Olsen, A.; Johannessen, T.; Croot, P. *Talanta* **2002**, *65*, 61.
(18) Schroeder, C.; Weidgans, B. M.; Klimant, I. *Analyst* **2005**, *130*, 907.
(19) Neurauter, G.; Klimant, I.; Wolfbeis, O. S. *Fresenius J. Anal. Chem.* **2000**, *366*, 481.
(20) Gouin, J. F.; Baros, F.; Birot, D.; Andre, J. C. *Sens. Actuators, B* **1997**, *39*, 401.
(21) Klimant, I.; Meyer, V.; Kuhl, M. *J. Limnol. Oceanogr.* **1995**, *40*, 1159.
(22) Song, A.; Parus, S.; Kopelman, R. *Anal. Chem.* **1997**, *69*, 863.

10.1021/cm060967n CCC: $33.50
Published on Web 08/16/2006

ment of (bio)chemical parameters. Fibers allow the optical information to be carried from the sample to the instrument. Optical sensing has a second feature that is not provided by electrochemical sensors: Sensing can be performed in a noncontact mode, for example, through the glass (or plastic) wall of a bioreactor. This is of particular advantage if sterility is an issue.

A substantial fraction of (fiber) optical sensors is based on the use of fluorescence as the optical information. This is due to the unsurpassed intrinsic sensitivity of fluorescence (that may reach the single-molecule level), and because certain effects (such as static/dynamic quenching or fluorescence resonance energy transfer) do occur in luminescence only. While the measurement of fluorescence intensity is simple in terms of instrumentation, its accuracy is often compromised by drifts in the optoelectronic setup (light sources and light detectors) and by variations of the properties of the sensor layer (e.g., the dye concentration or the thickness of the sensor layer). Therefore, referencing methods were developed for the precise measurement of fluorescence intensity.[24] One such method is based on the measurement of decay time which can be applied to indicator probes that undergo dynamic quenching (such as by oxygen) or undergo resonance energy transfer (which usually changes decay time as well).

The so-called dual lifetime referencing (DLR) method is relatively new and enables self-referenced measurements both in the time domain and in the frequency domain.[25,26] In contrast to the common ratiometric (i.e., 2-wavelength) method, this scheme uses luminophores with substantially different decay times. Usually, an analyte-insensitive phosphorescent reference dye (with a decay time in the microsecond range) is combined with an analyte-sensitive fluorophore (having a decay time in the nanosecond range).[27] It is essential for the DLR scheme to work so that the absorption and emission spectra of both indicators overlap to allow (a) simultaneous excitation of both probes with a single light source and (b) simultaneous detection of luminescence. In frequency domain DLR (fd-DLR), the combined luminescence intensity of both dyes is converted into a phase shift which is related to analyte concentration.

We perceived that a material for simultaneous sensing of pH and oxygen may be obtained if the analyte-insensitive reference luminophore is converted into an oxygen-sensitive luminescent indicator of similarly long decay time. In contrast to the conventional DLR method (in which phase shift is only dependent on pH), the overall phase shift in the resulting dual material now contains information on both species (pH and oxygen). If the phase shift is determined at two different modulation frequencies, two sets of information will be obtained that can be processed to give two specific analytical signals. The DLR methods rely on the fact that at higher modulation frequencies (but still in the kHz range) the long-lived luminescence undergoes demodulation, i.e., a decrease in intensity,[28] while the short-lived fluorescence (the one of the pH indicator) is not demodulated. A more detailed descripton of the modified DLR method used will be described elsewhere.

Since oxygen sensors based on the use of long-lived luminophores produce substantial quantities of singlet oxygen (which can deteriorate indicators), we further perceived that the use of microbeads (of 1−3 μm i.d.) for each indicator species would warrant a spatial separation of the indicators large enough to prevent photoinduced decomposition. We present our results on a novel optical dual sensor that makes use of the permeation-selective microbeads placed in a hydrogel and sensitive to either pH or oxygen. It is shown that the material enables simultaneous and noncontact measurement of pH and oxygen in physiological samples.

2. Experimental Section

Materials and Reagents. All chemicals and solvents were of analytical grade and were used without further purification. The preparation of ruthenium(II) tris-4,7-diphenyl-1,10-phenanthroline dichloride, referred to as $Ru(dpp)_3^{2+}$, has been described elsewhere.[29] It is commercially available from Alfa Aesar (www.alfa-chemcat.com). The pH indicator 5(6)-carboxyfluorescein (referred to as CF) and the chemicals *N*-(3-dimethylaminopropyl)-*N*′-ethylcarbodiimide hydrochloride (EDC), dimethylformamide, chloroform, triethylamine, and ethanol were purchased from Fluka (www.sigmaaldrich.com). Sodium 3-(trimethylsilyl)-1-propanesulfonate (Na-TMS; used as a lipophilic anion) was obtained from Aldrich (www.sigmaaldrich.com). The polyurethane hydrogel of type D4 was obtained from Cardiotech (www.cardiotech-inc.com), amino-modified polyacrylamide (AA-Q-N2), and amino-modified poly(hydroxyethyl methacrylate) (p-HEMA) from OptoSense (www.optosense.de). The chemically inert and optically transparent poly(ethylene terephthalate) support foils (type Mylar; 125 μm thick) were obtained from Goodfellow (www.goodfellow.com). Calibration gases (nitrogen and oxygen, each of 99.999% purity) were purchased from Linde (www.linde-gase.de). The preparation of organically modified sol−gel beads ("ormosil") was reported elsewhere.[30] The method used in the present work was similar to the method described[30] for material S1, the molar ratio of the monomers phenyltrimethoxysilane and tetramethoxysilane being 18:1. The ormosil polymer thus obtained possesses a porous structure, but its hydrophobic character (due to the presence of phenyl groups) prevents the penetration of charged species into the matrix. On the other side, the permeability for oxygen is improved (compared to sol−gels prepared from trialkoxysilanes).

Doubly distilled water was used for the preparation of the buffer solutions. Their pH was determined with a digital pH meter (Knick, www.knick.de) calibrated at 20 ± 2 °C with standard buffers of pH 7.0 and 4.0 (Merck; www.merck.de). The pH of solutions was adjusted to the desired value using MOPS buffers. These were adjusted to constant ionic strength (I = 25 or 140 mM) using sodium chloride as the background electrolyte.[31]

(23) Wolfbeis, O. S. *J. Mater. Chem.* **2005**, *15*, 2657.
(24) Park, E. J.; Reid, K. R.; Tang, W.; Kennedy, R. T.; Kopelman, R. *J. Mater. Chem.* **2005**, *15*, 2913.
(25) Klimant, I.; Huber, C.; Liebsch, G.; Neurauter, G.; Stangelmayer, A.; Wolfbeis, O. S. (edc) *Fluorescence spectroscopy: New Methods and Applications*; Springer: Berlin, 2001.
(26) Lakowicz, J. R.; Castellano, F. N.; Dattelbaum, J. D.; Tolosa, L.; Rao, G.; Gryczynski, I. *Anal. Chem.* **1998**, *70*, 5115.
(27) Liebsch, G.; Klimant, I.; Krause, C.; Wolfbeis, O. S. *Anal. Chem.* **2001**, *73*, 4354.
(28) Szmacinski, H.; Lakowicz, J. R. *Anal. Chem.* **1993**, *65*, 1668.
(29) Klimant, I.; Wolfbeis, O. S. *Anal. Chem.* **1995**, *67*, 3160.
(30) Klimant, I.; Ruckruh, F.; Liebsch, G.; Stangelmayer, A.; Wolfbeis, O. S. *Mikrochim. Acta* **1999**, *131*, 35.
(31) Perrin, D. D.; Dempsey, B. *Laboratory Manuals*; Chapmann & Hall: London, 1974; p 62.

Table 1. Probes and Materials (Plus Codes) Used for the Preparation of pH-Sensitive and O_2-Sensitive Membranes, and for the Dually Sensing Material[a]

code	indicator-loaded bead (SB) or bead-loaded sensor membrane (SM)	analyte
SB-1	$Ru(dpp)_3(TMS)_2$ in ormosil microbeads	O_2
SB-2	CF[b]) on p-HEMA microbeads	pH
SB-3	CF on AA-Q-N2 microbeads	pH
SM-1	$Ru(dpp)_3(TMS)_2$ in ormosil microbeads contained in an ~10-μm layer of hydrogel	O_2
SM-2	CF on p-HEMA microbeads suspended in an ~10-μm layer of hydrogel	pH
SM-3	CF on AA-Q-N2 microbeads suspended in an ~10-μm layer of hydrogel	pH
SM-4	SB-1 and SB-2 in an ~10-μm layer of hydrogel	O_2/pH

[a] All materials were deposited on an inert polyester support (see Figure 1A). [b] Carboxyfluorescein.

Preparation of Sensor Beads and Sensor Membranes. Materials were prepared for (a) sensing oxygen, (b) sensing pH, and (c) sensing both together. The following Table 1 summarizes the materials used for the various sensors. We differentiate between sensor beads (SB) and sensor membranes (SMs); SBs were contained in a hydrogel matrix. The membranes were obtained by spreading water/ethanol solutions of the sensor membrane material onto a solid transparent support (such as polyterephthalate or glass) and evaporating the solvent to give sensor membranes (SMs) at a thickness of ~10 μm.

Oxygen-Sensitive Microbeads (SB-1) and Sensor Membranes (SM-1). $Ru(dpp)_3^{2+}$ dichloride was converted into its much more lipophilic TMS salt by addition of an equivalent quantity of Na-TMS to an aqueous solution of the dye, followed by extraction of the $Ru(dpp)_3(TMS)_2$ ion pair into chloroform. Then, 200 mg of ormosil microparticles was dispersed in 20 mL of chloroform and 5 mg of the $Ru(dpp)_3(TMS)_2$ salt was added to the solution. A suspension of the ormosil polymer beads in chloroform was spread on a glass surface and dried at ambient air. After removal of the solvent, colored polymer film was mechanically ground, and the beads (SB-1) were washed several times with ethanol by centrifugation. A suspension of the polymer beads in ethanol was spread on a glass surface and dried at ambient air to give oxygen-sensitive beads SB-1.

To obtain membrane SM-1, 20 mg of the beads of type SB-1 was added to 600 mg of a 5 wt % solution of polyurethane hydrogel in an ethanol/water (9:1, v:v) mixture. The cocktail was spread as an approximately 120 μm thick film onto a 125 μm polyester support. After evaporation of the solvents, the orange-colored film had a thickness of 10 μm (as calculated from the masses employed).

pH-Sensitive Microbeads (SB-2, SB-3) and Sensor Membranes (SM-2 and SM-3). Carboxyfluorescein (CF) was covalently attached to the surface of the polymer particles using standard procedures.[32] Specifically, 300 mg of amino-modified p-HEMA was dispersed in 5 mL of water, and 5 mg of CF was added to the suspension. After the mixture was stirred for 10 min, 5 mg of EDC was added. The resulting suspension was stirred for another 2 h at room temperature. The particles were separated from the solution by centrifugation and washed several times with water, pH 4 buffer, pH 9 buffer, and ethanol until the washing remained colorless. The resulting beads were dried at ambient air to give material SB-2. A completely analogous procedure was applied to immobilize CF on the polyacrylamide beads to give sensor beads SB-3.

The preparation of the respective sensor membranes was similar to that of SM-1 in that 20 mg of beads of types SB-2 or SB-3 was added to 600 mg of a 5 wt % solution of polyurethane hydrogel in an ethanol/water (9:1, v:v) mixture. The cocktail was spread as an approximately 120 μm thick film onto a 125 μm polyester support. After evaporation of the solvents, the yellow films (of type SM-2 or SM-3) have a thickness of 10 μm.

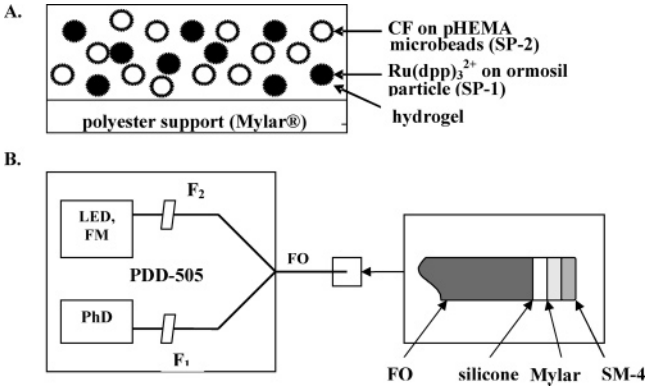

Figure 1. (A) Schematic of the sensor membrane SM-4 that is used for simultaneous optical sensing of oxygen and pH. The chemically sensitive materials are deposited on an inert mechanical support made from poly(ethylene glycol) (Mylar) that facilitates handling of the sensing films. (B) Optical setup and components used. LED, light-emitting diode; FM, frequency modulator; PhD, photodiode; F_1 and F_2, optical filters; FO, fiber optic cable; SM-4, sensor membrane that is glued to the tip of the fiber optic with silicone grease. The luminescence of the beads in membrane SM-4 is excited through the fiber, and a fraction of their total emission is guided back through the fibers to a photodiode detector where phase shifts are determined.

Dually Sensing Material (SM-4). To 20 mg of the pH-sensitive microbeads SB-2 and 10 mg of the oxygen-sensitive microbeads SB-1 was added 600 mg of a 5 wt % solution of the polyurethane hydrogel in an ethanol/water (9:1, v:v) mixture. This "cocktail" was stirred overnight, knife-coated (using a K Control Coater; see www.labomat.com) onto the polyester support, and dried at ambient air to obtain the yellow sensor membrane SM-4 in a thickness of about 10 μm.

Fiber Optic Dually Sensing Configuration. A spot of the sensor membrane SM-4 with a diameter of 2.0 mm was glued onto the tip of a 2-mm PMMA bifurcated fiber (from GP Fiber Optics; www.gp-fiberoptics.de). A cross section of the resulting film is shown in Figure 1A. The other ends of the fiber were attached to a 505-nm LED and to a photodiode, respectively. A schematic of the setup is given in Figure 1B.

Measurements. Fluorescence excitation and emission spectra as well as response curves of the sensor membranes were acquired with an Aminco-Bowman Series 2 luminescence spectrometer (SLM-Aminco, Rochester, NY; www.thermo.com) equipped with a homemade flow-through cell.[33] To spectrally characterize the sensor membranes, a 2-cm diameter spot was punched and placed in the cell. Buffer solutions (of varying pH and varying oxygen levels) were passed through the cell at a rate of 1 mL min^{-1} with the help of a Minipuls-3 peristaltic pump (Gilson, Vilers-Bel, France; www.gilson.com) via silicone tubing with an inside diameter of 1 mm.

Luminescence phase shifts of the fiber optic sensor (see Figure 1) were measured with a phase detection device PDD-505 (from Presens GmbH; www.presens.de). Light of a 505-nm LED is filtered through band-pass filter F_2 (505/60; from Analysentechnik; www.ahf.de). The dual luminescence of material SM-4 was filtered through a 570-nm long-pass filter F_1 (OG 570, Schott). The fiber sensor was immersed into a 100-mL glass beaker containing 30 mL of a buffer solution of defined pH. Nitrogen/oxygen gas

(32) Hermanson, G. T. *Bioconjugate Techniques*; Academic Press: New York, 1996; p 100.

(33) Huber, C.; Werner, T.; Krause, C.; Leiner, M. J. P.; Wolfbeis, O. S. *Anal. Chim. Acta* **1999**, *398*, 137.

Chart 1. Chemical Structures of the pH Probe Carboxyfluorescein (CF) and of the Oxygen Probe $Ru(dpp)_3^{2+}$ along with Its Counter Ion 3-Trimethylsilylpropane Sulfonate (TMS^-)

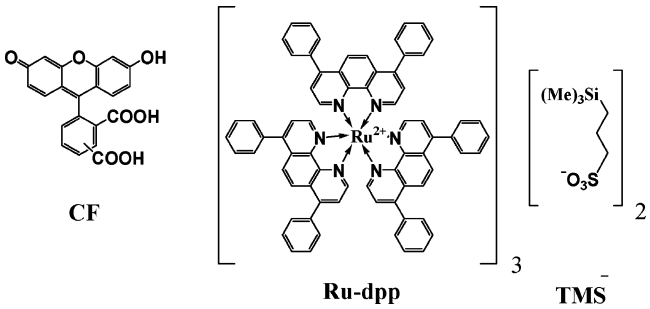

mixtures, whose composition and flow rate were controlled by a gas mixing device (GVS; from MKS; www.mksinst.com), were bubbled through the buffer solution to adjust the desired concentrations of dissolved oxygen. Temperature was kept constant at 20 °C by a RC 6 cryostat (Lauda; www.lauda.de). Photographic images of the sensor foil were acquired with a fluorescence microscope (Leica DMRE; Leica, www.leica.com), software ACD-Systems.

3. Results and Discussion

Choice of Materials. Simultaneous sensing of pH and oxygen via the modified DLR technique will work under the following conditions: (a) the oxygen indicator (which also serve as a reference luminophore) and the fluorescent pH indicator have to have largely different decay times; (b) each indicator has to respond to its analyte but may be cross-sensitive; (c) the excitation spectra of both indicators have to overlap in order to allow the simultaneous excitation of both indicators at a single wavelength; (d) the luminescence of both dyes is detectable at a single wavelength; (e) the ratio of the two components in a sensor cocktail must remain constant; and (f) the two luminophores ideally are compatible with an LED which is the preferred light source in practice.

We chose carboxyfluorescein (CF) as the pH indicator and ruthenium(II)-tris-4,7-diphenyl-1,10-phenanthroline [=$Ru(dpp)_3^{2+}$] as the oxygen indicator because they meet the above criteria. Carboxyfluorescein (CF), whose chemical structure is given in Chart 1, is highly fluorescent and a most common fluorescent acid−base indicator.[34] It covers the physiological pH range, and its pK_a is 6.5.[35] Its carboxy group can be used for covalent immobilization of the dye on the surface of amino-modified polymer particles in order to avoid leaching of the indicator, which can be a serious problem.[36]

CF was covalently immobilized on the surface of two kinds of polymer particles using standard procedures based on the peptide coupling reagent EDC.[32] The first polymer was a polyacrylamide derivative (referred to as AA-Q-N2) containing 4% of *N*-(3-aminopropyl)acrylamide which provides free amino groups for attachment of carboxyfluorescein. The second is a derivative of poly(hydroxyethyl methacrylate), also referred to as p-HEMA, which also contains primary amino groups due to the presence of 4% of *N*-(3-aminopropyl)acrylamide. Both materials possess excellent mechanical, chemical, and thermal stability and do not dissolve in any solvents, but differ significantly in their hydrophobic properties. Aminocellulose was another choice for a polymer matrix but was not employed because it is an excellent nutrient for certain bacteria.

To facilitate handling and characterization of the sensor materials, they were deposited as thin (10 μm) films on a solid support. Poly(ethylene glycol terephthalate), the material used as a support in conventional photographic films, has been used for years by us (and others) as a support for sensor layers since it is mechanically stable, can be punched or cut on various sizes and shapes, has excellent optical transparency, is completely inert (both chemically and spectroscopically, except for a weak blue luminescence if excited at below 400 nm), and is readily available.

The oxygen sensor material makes use of the ruthenium(II) complex $Ru(dpp)_3^{2+}$ (Chart 1). This indicator benefits from fairly strong absorption in the visible region (λ_{max} = 463 nm, $\epsilon = 2.84 \times 10^4$ $M^{-1}\cdot cm^{-1}$), a good luminescence quantum yield (QY) of 0.36,[37] and thus a good brightness (*Bs*; defined as $\epsilon\cdot$QY) which is 10200 $M^{-1}\cdot cm^{-1}$. It also exhibits good photostability.[38] In the complete absence of oxygen, $Ru(dpp)_3^{2+}$ has a decay time on the order of 3−5 μs (depending on the polymer "solvent" used) and can serve as an excellent oxygen probe when contained in a highly oxygen-permeable polymer.[39−41] We had discovered[30] a highly oxygen-permeable type of ormosils that can be prepared in the form of microbeads with a diameter of 1−3 μm.[42,43] The indicator $Ru(dpp)_3^{2+}$ was incorporated into the polymer beads by swelling them in a chloroform solution. The material was then deposited on the polyester support to obtain a.

The sensor for simultaneous sensing of pH and oxygen contains both kinds of beads embedded in a single polymer matrix deposited on the polyester support. Hydrogels (which are permeable to both protons and oxygen) have excellent mechanical properties and excellent stability at various pHs.[44] The polyurethane-based hydrogel used here has excellent water uptake (and thus swells) and is biocompatible. Sensor membranes made from beads of type SB-2 (based on p-HEMA), according to visual inspection, possessed higher brightness than those made with beads SB-3. Thus, we prefer material SM-2 in the dual sensor.

Response of the pH-Sensor Materials SM-2 and SM-3. In most biotechnological applications it is necessary that the pK_a values of a pH-sensitive probe be around 7. The

(34) Elliad, R. S.; Tuvia, S. *New J. Chem.* **1999**, *23*, 1187.
(35) Haugland, R. P. *Handbook of fluorescent probes and research products*; Molecular Probes Inc.: 2002; Chapter 21 (www.probes.com).
(36) Butler, T. M.; MacCraith, B. D.; McDonagh, C. J. *Non-Cryst Solids* **1998**, *224*, 249.
(37) Alford, P. C.; Cook, M. J.; Lewis, A. P.; McAuliffe, G. S. G.; Skarda, V.; Thomson, A. J. *J. Chem. Soc., Perkin Trans II* **1985**, 705.
(38) Xu, H.; Aylott, J. W.; Kopelman, R.; Miller, T. J.; Philbert, M. A. *Anal. Chem.* **2001**, *73*, 4124.
(39) Morin, A.; Xu, W.; Demas, J.; DeGraff, B. *J. Fluoresc.* **2000**, *10*, 7.
(40) Mongey, K. F.; Vos, J. G.; MacCraith, B. D.; McDonagh, C. M.; Coates, C.; McGarvey, J. J. *J. Mater. Chem.* **1997**, *7*, 1473.
(41) McEvoy, A.; McDonagh, C.; MacGraith B. *J. Sol-Gel Sci. Technol.* **1997**, *8*, 1121.
(42) Fröba, M.; Köhn, R.; Bouffaud, G.; Richard, O.; Van Tendeloo, G. *Chem. Mater.* **1999**, *11*, 2858.
(43) Wang, H.; Chen, P.; Zheng, X. *J. Mater. Chem.* **2004**, *14*, 1648.
(44) Peppas, N. A. *Preparation Methods & Structures of Hydrogels*; CRC Press: Boca Raton, FL, 1986.

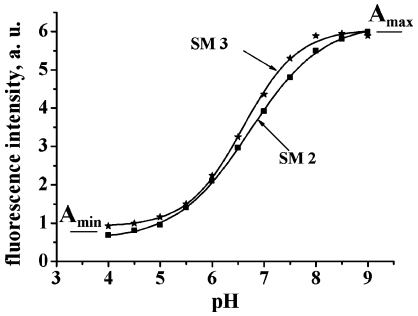

Figure 2. Response curves of materials SM-2 and SM-3 to pH. The indicator CF is excited at 490 nm. The ionic strength of the buffers was kept constant at 140 mM.

apparent pK_a value of an indicator in a polymer depends on not only its intrinsic (thermodynamic) pK_a value but also the kind of polymer used. Two different dye−polymer combinations (materials SM-2 and SM-3) were investigated. Figure 2 shows response of the probes to pH. Sensor membranes SM-2 and SM-3 display good pH sensitivity in range from pH 5 to pH 8.

The curves can be described quite well (with a correlation coefficient of 0.999) by the following equation, adapted earlier[45] for optical pH sensors

$$I = \frac{A_{\max} - A_{\min}}{1 + 10^{(\mathrm{pH}-\mathrm{pK_a})/x}} + A_{\min} \qquad (1)$$

where I is fluorescence intensity and A_{max}, A_{min}, and x are numerical coefficients. The equation gave pK_a values of 6.71 and 6.58, respectively, for materials SM-2 and SM-3. A_{max} and A_{min} are numerical values of the fluorescence intensity of the pH indicator in fully protonated (A_{min}) and fully deprotonated (A_{max}) form, respectively.

Any polymer used as a matrix for immobilizing pH indicators has three kinds of effects on the properties of the pH indicator: The first is on the pK_a value, the second on the spectra (shape and peaks), and the third on the shape of the response curves which for polymer-immobilized indicators mostly are different from those obtained for solutions. Indeed, the pK_a values are slightly higher for the immobilized form of the dye compared to the one in aqueous solution ($pK_a = 6.5$). A similar, but larger effect was found when fluorescein[46] was covalently attached to differently charged surfaces of certain polymers. Most likely, this is the result of the varying density of electrical charges on the surface. Usually, a rather small increase in pK_a occurs on covalent[47] or electrostatic[48] immobilization of an indicator even to nonionic polymers, a fact that is attributed to the decrease in the polarity of the microenvironment.

The spectra of membrane SM-2 are different from the respective spectra of CF in solution. While fluorescence intensity, as expected, drops strongly on going from pH 9 to pH 4, the fluorescence of CF in p-HEMA peaks at 530 nm and thus is strongly bathochromically shifted (compared to CF in aqueous solution which has a λ_{max} of 517 nm at pH 9). The effect is assumed to be caused by a decrease in the polarity of the microenvironment, but also by different hydration of the immobilized indicator. A similar behavior was observed earlier for immobilized fluorescein.[49,50]

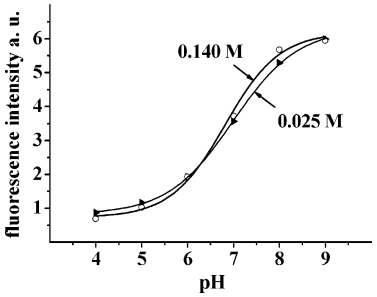

Figure 3. Titration curves for sensor membrane SM-2 at ionic strengths of 25 and 140 mmol L^{-1} adjusted with NaCl. Fluorescence was excited at 490 nm, and emission intensity was measured at 530 nm.

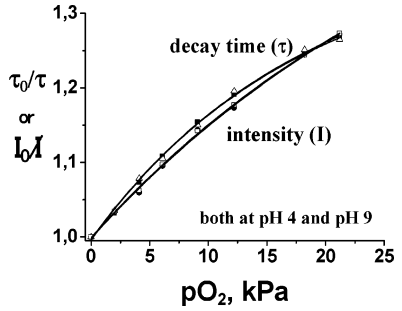

Figure 4. Lifetime-based and intensity-based Stern−Volmer plots obtained for the oxygen-sensitive microbeads dispersed in hydrogel (material SM-1) at two pH values. The plots for pH 4 and 9 overlap completely, this demonstrating the insensitivity to pH.

One disadvantage of optical pH sensors is the adverse effect of ionic strength (IS) on the dissociation constant and, consequently, the pK_a of the dye.[51,52] The effect of IS cannot be distinguished from signal changes caused by pH and therefore can compromise sensor performance. Figure 3 shows titration curves for the pH sensor SM-2 at two ISs (25 and 140 mM). The latter represents the upper limit of IS in most physiological solutions including blood. The pK_a decreases slightly (from 6.89 to 6.81 on going from 25 to 140 mM). Thus, the cross sensitivity of SM-2 to IS is surprisingly small.

The response time t_{95} (i.e., the time for 95% of the total change in fluorescence intensity to occur) to altering the pH was not exceeding 1 min on going from pH 4 to pH 9 and 1.5 min in the reverse direction. The values are in good agreement with those obtained for other optical pH-sensitive materials based on the sol−gel silica matrix.[51]

Response of the Oxygen Sensor Membrane SM-1. Figure 4 shows the response curve for an oxygen sensor film made from SM-1 at two pH values. Strictly speaking, the probe responds to dissolved oxygen. However, for the sake

(45) Weidgans, B. M.; Krause, C.; Klimant, I.; Wolfbeis, O. S. *Analyst* **2004**, *129*, 645.
(46) Agi, Y.; Walt, D. R. *J. Polym. Sci., A: Polym. Chem.* **1997**, *35*, 2105.
(47) Kostov, Y.; Tzonkov, S.; Yotovan, L.; Krysteva, M. *Anal. Chim. Acta* **1993**, *280*, 15.
(48) Jones, T. P.; Porter, M. D. *Anal. Chem.* **1988**, *60*, 404.
(49) Fuh, M.-R. S.; Burgess, L. W.; Hirschfeld, T.; Christian, G. D. *Analyst* **1987**, *112*, 1159.
(50) Sanchez-Barragan, I.; Costa-Fernandez, J. M.; Sanz-Medel, A. *Sens. Actuators B* **2005**, *107*, 69.
(51) Leiner M. J. P.; Wolfbeis, O. S. In *Fiber Optic Chemical Sensors and Biosensors*; Wolfbeis, O. S., Ed.; CRC Press: Boca Raton, FL, 1991; p 63.
(52) Leiner, M. J. P.; Hartmann, P. *Sens. Actuators B* **1993**, *11*, 281.

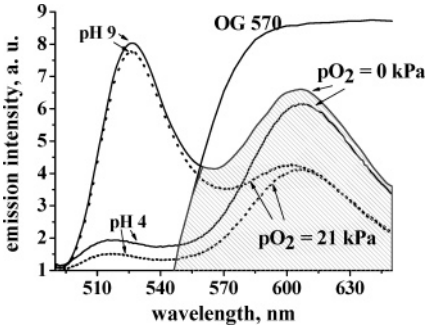

Figure 5. Emission spectra of the indicators in the dual sensor (CF/p-HEMA and $Ru(dpp)_3^{2+}$/ormosil microbeads dispersed in hydrogel, λ_{exc} = 470 nm) at various pHs and oxygen partial pressures. Included are the spectral cutoffs of the absorbance filter used. The hatched area represents the luminescence of the indicators that passes the long-pass filter (OG 570) and is detected by the photodetector.

of simplicity we prefer to use oxygen partial pressure above the buffer solution. It is proportional to the concentration of the dissolved gas according to Henry's law.

The decay times of SM-1 were calculated using eq 4 by measuring Φ at two modulation frequencies (f_1 = 30 kHz; f_2 = 60 kHz). The calculated luminescence decay time in the absence of oxygen was 5.4 μs. As can be seen from Figure 4, intensity and lifetime Stern−Volmer plots are quite similar. It can also be seen that sensitivity to oxygen is independent of pH.

The response to oxygen is very fast: a change from deoxygenated water to air-saturated water is indicated within 6 s (t_{95}, the time for 95% of the total signal change to occur). The t_{95} for the reverse direction was 7 s only. Although even faster sensors have been reported,[30,53] the response of our probe is faster than that of other sol−gel materials.[41,54] pH has no effect at all (Figure 4).

Response of the Dual Sensor in the Intensity Mode. In the pH/oxygen dual sensor, the fluorescence of the pH indicator is referenced against the phosphorescence of the oxygen indicator. Too low a sensitivity will result in higher error in oxygen partial pressure, but also in calculated pH values. On the other side, if sensitivity to oxygen is too high, the overall phase shifts in dual sensor will be too low at oxygen saturation, resulting in low precision of pH sensing under this condition. The $Ru(dpp)_3^{2+}$/ormosil oxygen-sensitive microbeads, thus, allow optimal sensitivity to oxygen.

In the dually sensing material SM-4 both kinds of the microbeads (SB-1 and SB-2) are contained in a single polymer matrix. The absorption spectra of CF (with a λ_{max} of 490 nm) and $Ru(dpp)_3^{2+}$ (λ_{max} 470 nm) strongly overlap, and this enables excitation of both indicators by the 505-nm (blue-green) LED.

The emission spectra of the two indicators are shown in Figure 5. The fluorescence intensity of the pH indicator CF is weak at pH 4 and high at pH 9. The emission of the oxygen-sensitive probe is not affected by pH. If the oxygen partial pressure is increased, the emission intensity of $Ru(dpp)_3^{2+}$ decreases, while that of the pH indicator decreases

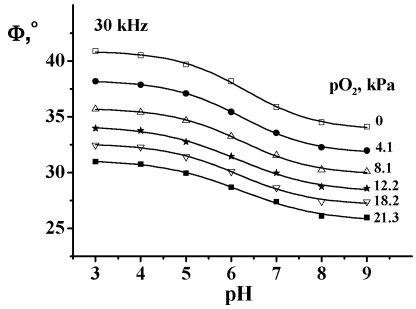

Figure 6. pH dependence of the phase shift at 30 kHz in the dual sensor at various oxygen partial pressures (in gas equilibrated buffer solution). Lines represent a fit via eq 1.

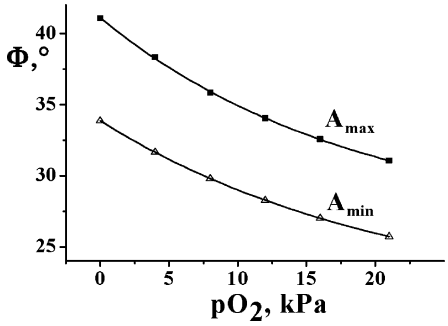

Figure 7. Dependence of the parameters A_{max} and A_{min} on oxygen concentration at a modulation frequency of 30 kHz. Lines represent fits via eq 2 (the monoexponential decay model).

by around 4% only (on going from pure nitrogen to pure oxygen at constant pH). Generally, the emission intensities at 530 and 610 nm and the decay time of the long-lived luminophore should be measured. The intensity of fluorescence is then referenced to the decay time.

Response of the Dual Sensor to pH in the Frequency Domain. In the conventional DLR type of sensor, the fluorescence of a pH indicator is related to the luminescence intensity of a completely inert long-lived reference luminophore. The behavior of such a sensor can be described by a single calibration curve (phase shift Φ vs pH), which is very similar to that presented in Figure 6 (measured in the absence of oxygen). The long-lived inert reference luminophore of such sensors typically is contained in a gas-impermeable polymer (usually in the form of polyacrylonitrile microbeads[18]) and thus remains unaffected by oxygen. In the frequency-domain DLR method the emission of both indicators is measured simultaneously, which is achieved by using a 570-nm long-pass filter (Figure 5). The shaded area represents the part of the emission which passes the filter and is registered by the photodetector.

The situation becomes more complicated if the reference luminophore is substituted by an oxygen indicator. Now, the overall phase shift depends on the concentrations of both analytes (Figure 6). We chose a modulation frequency of 30 kHz, and this resulted in the work functions for pH shown in Figure 6. They show that the response curves of pH indicator have similar shapes at different oxygen concentrations (pO_2 from 0 to 21.3 kPa).

For given oxygen level the plots are well described by eq 1. Fitting gives a pK_a of 6.21 and x is 1.932, both parameters being independent of oxygen partial pressure. The fit parameters A_{min} and A_{max}, on the other side, reflect contribu-

(53) McNamara, K. P.; Li, X.; Stull, A. D.; Rosenzweig, Z. *Anal. Chim. Acta* **1998**, *361*, 73.
(54) Garcia-Fresnadillo, D.; Marazuela, M. D.; Moreno-Bondi, M. K.; Orellana, G. *Langmuir* **1999**, *15*, 6451.

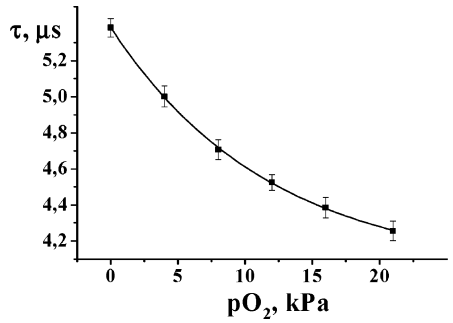

Figure 8. Response function of the dual sensor toward oxygen at pH 3, pH 4, pH 5, pH 6, pH 7, pH 8, and pH 9. The data practically overlap completely. The square data points are the decay times as calculated via eq 4. The line represents a fit via eq 2.

tion of the luminescence of the oxygen probe (which is quenched) to the overall phase shift.

The plots could be well described by algorithms identified with the Table Curve 2D software. The resulting equations characterize the plots for the parameters A_{max} and A_{min} vs the oxygen partial pressure (Figure 7) by a monoexponential decay model (standard deviation $r^2 = 0.99965$)

$$y = B \cdot e^{(-(pO_2/C))} + D \quad (2)$$

where y is the phase shifts in the deprotonated (A_{max}) and protonated (A_{min}) forms and B, C, and D are fit parameters.

The following fit parameters were thus obtained from eq 2: $B_{max} = 14.817$, $C_{max} = 18.580$, and $D_{max} = 26.281$ for A_{max}, and $B_{min} = 12.984$, $C_{min} = 21.331$, and $D_{min} = 20.878$ for A_{min}. The equations describing dependence of A_{max} and A_{min} (eq 2) are thus indroduced into eq 1 to obtain, after mathematical conversion, the following equation for calculation of pH:

$$pH = 6.208 + \ln\left(\frac{(B_{min}\exp(-pO_2/C_{min}) + D_{min}) - \Phi_{30kHz}}{\Phi_{30kHz} - (B_{max}\exp(-pO_2/C_{max}) + D_{max})}\right) \times 0.8387 \quad (3)$$

Response of the Dual Sensor to Oxygen in the Frequency Domain. One way to describe the response of the sensor to oxygen is to use the formula for compensation of the background fluorescence.[55] The equation was used for screening the fluorescence of pH indicator in the dual sensor. The phase shifts are measured at 30 kHz (f_1) and 60 kHz (f_2). The fluorescence of pH indicator does not affect the decay time of the long-lived luminophore calculated according to eq 4 (obtained via eq 1) at two different frequencies

$$\tau = \frac{1}{2\pi}\left(\frac{f_1^2 - f_2^2 \pm \sqrt{f_2^2 - f_1^2 - 4(\cot\Phi_2 \cdot f_2 \cdot f_1^2 - \cot\Phi_1 \cdot f_1 \cdot f_2^2)(\cot\Phi_2 \cdot f_2 - \cot\Phi_1 \cdot f_1)}}{2(\cot\Phi_2 \cdot f_2 \cdot f_1^2 - \cot\Phi_1 \cdot f_1 \cdot f_2^2)}\right) \quad (4)$$

where Φ_1 and Φ_2 are the phase shifts at modulation frequencies f_1 and f_2.

The equation enables the calculation of the decay times of long-lived luminescent indicators in the presence of another fluorescent dye. Overall phase shifts measured at 30 and 60 kHz in the absence of oxygen (see Figure 6) depend on pH since the luminescence of the pH indicator contributes to the overall phase shift. However, if eq 4 is used, the decay time calculated for the oxygen indicator ($\tau_0 = 5.38 \pm 0.05$ μs) remains constant from pH 3 to pH 9.

(55) Neurauter, D. Ph.D. Thesis. University of Regensburg, Regensburg, 2000; p 106.

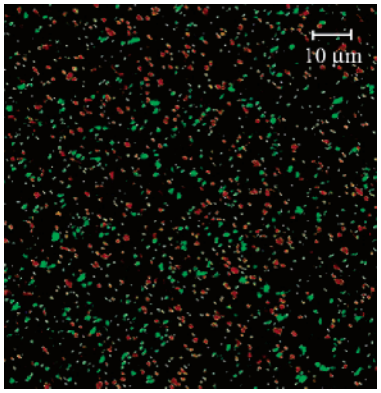

Figure 9. Photographic image of the sensor membrane SM-4 soaked with a saturated aqueous pH 8 solution of Na_2SO_3 (in order to remove all dissolved oxygen) and showing two kinds of fluorescent particles. Those with red luminescence are ormosil-based and incorporate the oxygen probe $Ru(dpp)_3^{2+}$. Those with green fluorescence are based on poly(hydroxyethyl methacrylate) and contain carboxyfluorescein which responds to pH.

The response function of the dual sensor toward oxygen is presented in Figure 8. Again, eq 2 was used for fitting (correlation coefficient $r^2 = 0.999$) and the following fit parameters were obtained: $B = 1.354 \times 10^{-6}$, $C = 11.956$, and $D = 4.031 \times 10^{-6}$. The oxygen concentration can be calculated via the following eq 5

$$pO_2 = -C \ln\left(\frac{\tau - D}{B}\right) \quad (5)$$

where τ is the decay time calculated via eq 4. While this equation nicely matches the response function, it is obvious that a (tedious) multipoint calibration is needed for such kind of sensors.

Sensor Homogeneity. The homogeneity of the materials is very important for any sensor making use of the m-DLR technique along with bead indicators since good spatial resolution of calibration plots can be compromised by such inhomogeneities. Figure 9 shows a photographic image of a sensor membrane (SM-4) taken on a fluorescent microscope. To avoid aggregation of the particles, their concentration (at the same mass ratio of SB-1 to SB-2) in the hydrogel was reduced by a factor of 10. The size of both the pH-sensitive (green fluorescent) particles and of the oxygen-sensitive (red fluorescent) particles is estimated to range between 1 and 3 μm.

The size of the microparticles is indeed sufficient to obtain a highly homogeneous sensor layer for measurements using a 2-mm fiber optic and possibly also is adequate for fiber tips as thin as 100 μm only. This was proven by measurement of the phase shifts (at pH 8 and zero pO_2) of seven randomly chosen spots of 2 mm diameter punched from a 20 $\times$ 30 mm piece of sensor foil. The standard deviation of the phase shift Φ at a modulation frequency of 60 kHz is higher ($\Phi = 41.17 \pm 0.19$) than that at a frequency of 30 kHz ($\Phi = 33.56 \pm 0.07$); however, it does not exceed 0.45%.

Table 2. Determination of the pH and pO_2 (in kPa Units) by the Dual Sensor in Test Solutions (at Room Temperature)

solution no.	analyte	adjusted values	calc. values	solution no.	analyte	adjusted values	calc. values
1	pO_2	5.10	5.70	4	pO_2	5.10	5.87
	pH	6.50	6.60		pH	4.46	4.49
2	pO_2	15.20	16.19	5	pO_2	15.20	16.79
	pH	6.50	6.43		pH	4.46	4.23
3	pO_2	5.10	5.61	6	pO_2	15.20	16.44
	pH	7.53	7.38		pH	7.53	7.72

Validation. The response functions were validated with test solutions of pH 7.53, 6.50, and 4.46, respectively. They were equilibrated with oxygen to give a pO_2 of 5.10 and 15.20 kPa, respectively. Phase shifts were then determined at 30 and 60 kHz. The data obtained were used to calculate the oxygen concentration via eq 5 and introduced into eq 3 to obtain the pH value. Table 2 compares the calculated and real values of pH and pO_2. The deviation between real and calculated pO_2 does not exceed 15%, while the highest error in pH determination is 0.23 units. One can observe, however, that the calculated pO_2 is always slightly higher than the pO_2 applied. This systematic error is most likely due to the difference in the temperatures when calibrating (20 °C) and when validating (23 °C) the sensors, a fact that unfortunately was discovered after the completion of the experiments only. It is known[56,57] that the sensitivity of this oxygen probe increases with temperature.

4. Conclusion

New sensor materials are introduced that enable simultaneous sensing of pH (between 4 and 9) and dissolved oxygen (pO_2; between 0 and air saturation). Fluorescent indicators are immobilized in different kinds of organic-polymer microbeads (ormosil, amino-modified polyacrylamide, and amino-modified poly(hydroxyethyl methacrylate), respectively), which in turn are contained in a hydrogel matrix. This approach displays significant advantages over sensor materials with homogeneously dissolved indicators in that (a) the selectivity and sensitivity of indicators can be controlled, (b) cross-sensitivities (e.g., because of quenching) can be reduced to a minimum, and (c) the system is more photostable because the singlet oxygen produced in the oxygen beads cannot decompose the pH indicator contained in the other beads. Sol−gels have been used successfully in sensors before[58] but are used here preferably for preparation of the oxygen microbeads in order to impart selectivity, stability, and adequate amphiphilicity to retain the oxygen indicator.

Acknowledgment. We thank the German Federal Ministry of Education and Research (BMBF) for financial support (project Biophotonik BP28).

CM060967N

(56) Demas, J. N.; DeGraff, B. A. *Sens. Actuators B* **1993**, *11*, 35−41.
(57) Ogurtsov, V. I.; Papkovsky, D. B. *Sens. Actuators B* **2006**, *113*, 917−929.
(58) Wolfbeis, O. S.; Reisfeld, R.; Oehme, I. *Struct. Bonding (Berlin)* **1996**, *85* (Optical and Electronic Phenomena in Sol−Gel Glasses), 51−98.